Life Sciences 232 (2019) 116632

Contents lists available at ScienceDirect

Life Sciences

journal homepage: www.elsevier.com/locate/lifescie

miRNA-181a over-expression in mesenchymal stem cell-derived exosomes influenced inflammatory response after myocardial ischemia-reperfusion injury

Wei Zilun[a,1], Qiao Shuaihua[b,1], Zhao Jinxuan[b,1], Liu Yihai[a], Li Qiaoling[b], Wei Zhonghai[b], Dai Qing[b], Kang Lina[b], Xu Biao[b,*]

[a] Department of Cardiology, Nanjing Drum Tower Hospital, Clinical College of Nanjing Medical University, Nanjing 210008, China
[b] Department of Cardiology, Nanjing Drum Tower Hospital, Nanjing University Medical School, Nanjing 210008, China

ARTICLE INFO

Keywords:
miRNA-181a
Inflammation
Regulatory T cell
C-Fos
Myocardial infarction
Bioinformatics

ABSTRACT

Aims: The inflammation modulation effects of mesenchymal stromal cell-derived exosomes (MSC-EXO) are well established. We aimed to explore the mechanism behind the inflammatory responses of numerous exosomal cargo molecules that have been neglected in molecular biology research, and to develop an exosomal cargo delivery system that can exert a stronger therapeutic effect on myocardial ischemia-reperfusion (I/R) injury.

Main methods: Computational approaches were used to identify key exosomal miRNAs and their downstream mRNAs that are expressed in the inflammatory response. Direct interactions between miRNA-181a and the c-Fos mRNA complex were confirmed by luciferase reporter assay. MSC-EXO carrying miRNA-181a-overexpressing lentiviruses were intramyocardially injected into a mouse model of myocardial I/R injury. I/R progression was evaluated through echocardiography and immunofluorescence microscopy.

Key findings: miRNA-181a provided substantial coverage against a host of immune-related genes through the miRNA-mRNA network. miRNA-181a delivery by MSC-EXO combined the immune-suppressing effect of miRNA-181a and the cell targeting capability of MSC-EXO to exert a stronger therapeutic effect on myocardium I/R injury.

Significance: We showed the potential of MSC-EXO as a tool for the specific delivery of small RNAs in vivo. This study shed new light on the potential application of miRNA-181a-overexpressing MSC-EXO as a therapeutic strategy for myocardial I/R injury.

1. Introduction

Myocardial infarction, which leads to cardiac remodeling and subsequent heart failure, is a common and prevalent disease. Although timely reperfusion and concomitant reoxygenation can reduce the infarct size to a large extent, patients surviving a myocardial infarction are still faced with a poor prognosis owing to their worsened cardiac function and the aggravated progression of heart failure [1]. The myocardial ischemia-reperfusion (I/R) process often starts an inflammatory cascade in the heart [2]. The high expression of pro-inflammatory mediators may be a cause of the further loss of cardiomyocytes by activating the pro-apoptotic pathways [3,4]. Regulatory T (Treg) cells, a subtype of T cells, are produced in the thymus or peripheral lymphoid organs before entering the blood circulation [5]. By inhibiting cardiomyocyte apoptosis and acting as a check against unrestrained inflammation through the amelioration of both inflammatory cell infiltration and macrophage polarization via direct contact and paracrine effects, exogenous Treg cell transplantation has shown huge potential in alleviating myocardial I/R injury [6,7]. Hence, the strengthened containment of the inflammatory response is important for infarct healing [8].

Some target genes have been shown to play an important role in regulating the inflammatory and repair responses after myocardial ischemia [9,10]. Experiments have revealed that miRNAs play an irreplaceable role in modulating systemic and local immunologic imbalances as well as the pathogenesis of cardiovascular diseases, the focus of this present study [11–13]. Dysregulation of the miRNA-181a expression level was found in inflammatory-related diseases [14,15]

* Corresponding author.
E-mail address: xubiao62@nju.edu.cn (B. Xu).
[1] Contributed equally.

https://doi.org/10.1016/j.lfs.2019.116632
Received 22 May 2019; Received in revised form 29 June 2019; Accepted 3 July 2019
Available online 03 July 2019

and unstable angina (GSE49823, Chen H). Gene Ontology (GO) computational simulations suggested targets of miRNA-181a to be highly enriched in T-cell receptor signaling and transforming growth factor-beta (TGF-β) signaling [16], which plays a key role in Treg cell activation. Moreover, miRNA-181a could attenuate *oxidized* low-density lipoprotein (ox-LDL)-stimulated dendritic cell (DC) activation and inflammatory responses in a c-Fos-dependent manner. Since many studies have suggested that TGF-β play an important role in modulating FoxP3 expressions, a main regulator of Treg cells, at the protein and mRNA levels in vivo and in vitro [17–19], we implemented this present study to demonstrate the immunomodulatory effect of miRNA-181a on inflammatory factors and Treg cell polarization in a mouse model of myocardial I/R injury.

An unstable miRNA molecular structure would be rapidly degraded after entering the systemic circulation and must therefore rely on a stable carrier to further exert its biological effects [20,21]. Exosomes have been suggested to serve as possible drug delivery vehicles owing to their nanometer-size range and capability of transferring biological materials to recipient cells [22]. A majority of studies have exploited exosomes for the transfer of endogenous or exogenous miRNA cargo [22]. Mesenchymal stromal cells (MSCs) have been reported to exert profound immunoregulatory effects on DCs, Treg cells, and monocytes or macrophages via paracrine effects, indicating that exosomes derived from MSCs (MSC-EXO) have high affiliation with these immune cells [23–27]. Hence, we hypothesized that miRNA-181a delivery by MSC-EXO would combine the immune suppressive effect of miRNA-181a and the cell targeting capability of MSC-EXO to exert a stronger therapeutic effect on myocardial I/R injury. In this study, we used lentiviruses as the vectors for mediating the miRNA-181a overexpression in MSC-EXO. Treatment with the miRNA-181a-overexpressing MSC-EXO significantly improved the cardiac function and reduced the infarct sizes in mice with myocardial I/R injury. Additionally, it was found that the treatment had created an anti-inflammatory environment and increased Treg cell polarization through the downstream c-Fos protein.

2. Materials and methods

2.1. In silico analysis

The gene expression profiles of the Gene Expression Omnibus (GEO) datasets GSE78865 and GSE49823 were downloaded from the GEO database (https://www.ncbi.nlm.nih.gov/) [28]. GSE78865 is based on the GPL13987 platform (TaqMan Array Human MicroRNA A Card v2.0, Applied Biosystems, USA), which comprises the human bone marrow stromal cell-derived exosomal miRNA profiles of samples obtained from 2 young patients, 2 elderly patients, and 2 patients with multiple myeloma (submission date March 3, 2016; last updated May 12, 2017). In this present research, exosome-harbored candidate miRNAs from these six patient samples that were found by the GEO2R tool to not have differentially expressed levels were picked up for further study. The major inclusion criterion was $P > 0.05$, which was completely opposite to the normal analysis of differentially expressed genes. The sequence and identity of miRNA-181a were provided through the miRWalk database, with a target score of ≥90 (http://zmf.umm.uni-heidelberg.de/apps/zmf/mirwalk2/). The expression profiles of miRNA-181a in the different tissues were determined using the GEO dataset GSE49823, which is based on the GPL15467 platform (TaqMan Human MicroRNA Array v3.0 A/B, Applied Biosystems, USA). Genes putatively targeted by miRNA-181a were identified using miRWalk, TargetScan (http://www.targetscan.org), PicTar (http://www.pictar.org/), and starBase (http://www.pictar.org/). Overlapping target genes were established. GO and Kyoto Encyclopedia of Genes and Genomes (KEGG) pathway enrichments of the candidate genes were carried out using the online tool Database for Annotation Visualization and Integrated Discovery (https://david.ncifcrf.gov/) and FunRich software (v3.3, http://www.funrich.org/). A threshold of $P < 0.05$ was used to identify functional enrichment. The highest 10 to 20 enriched biological process and molecular function terms were illustrated. Protein-Protein Interaction Network data were obtained from the Search Tool for the Retrieval of Interacting Genes (STRING) database (http://string-db.org), and interactions among the candidate genes were visualized using Cytoscape software (v3.6.1, http://www.cytoscape.org/). Proteins that have more interactions with adjacent proteins are much more likely to be encoded by a hub gene. The ClueGO plug-in from the Cytoscape App Store (http://apps.cytoscape.org/apps/cluego) is updated with the newest files from GO, KEGG, WikiPathways, and Reactome. In this study, ClueGO was used to reveal the different signaling pathways and relevant proteins that are obviously modulated by miRNA-181a.

2.2. Cell culture

Clinical-grade human umbilical cord blood-derived MSCs were isolated and obtained from the Stem Cell Laboratory of Drum Tower Hospital and cultured in MSC medium (#7501, ScienceCell, USA) containing 5% exosome-depleted fetal bovine serum (FBS) (C38010050, BioInd, Israel), 1% MSC growth supplement, and 1% penicillin/streptomycin solution. The MSCs were cultured to 3–8 passages at 37 °C in a humidified incubator under 10% CO_2. Once the cells had reached approximately 80% confluency, they were digested with 0.125% trypsin-EDTA (ZS807-3, OMANBIO, China), seeded into T225 culture bottles with 20 ml of new medium, and incubated for 72 h to obtain exosomes. The proliferation and morphology of the MSCs were monitored continuously.

Peripheral blood mononuclear cells (PBMCs) were obtained from fresh whole blood of healthy, anonymous donors with paroxysmal supraventricular tachycardia and without a history of coronary heart disease, permanent pacemaker implantation, or fever symptom. All donors provided their informed consent for inclusion in the study before their participation. The study was conducted in accordance with the Declaration of Helsinki, and the protocol was approved by the Institutional Ethics Committee of Nanjing Drum Tower Hospital (Approval No. 20011147). Volunteers were recruited from the Department of Cardiology, Drum Tower Hospital, Nanjing, China, with complete ethical consent in writing [see Additional file 1]. The PBMCs were collected from 4 ml of sodium heparinized blood per tube and then diluted 1:1 in bacteria-free phosphate-buffered saline (PBS). After lymphocyte separation medium (70-LSM02, Multisciences, China) treatment and gradient centrifugation, the white ring layer containing the PBMCs was collected and plated on a 12-well culture plate (020012, Sybio, China) at the density of 2×10^6 to 5×10^6 cells/well, following which RPMI 1640 medium (P0201-01, Biogene, USA) containing 10% FBS (11011-8611, EVERY GREEN, China) was added. The PBMCs were harvested after 72 h of incubation with the miRNA mimics or MSC-EXO.

2.3. Lentivirus vector construction and cell transduction

To produce miRNA-181a-expressing lentiviruses, the GV309 expression vector (GeneChem, China) was used. The human miRNA-181a gene sequence (NR_029611.1) was obtained from GenBank (http://www.ncbi.nlm.nih.gov/genbank/) and a scrambled sequence (TTC TCC GAA CGT GTC ACG T) was created as a negative control construct (control miRNA) that should have no homology with the human genome. The target gene was amplified by the polymerase chain reaction (PCR) using the forward primer 5′-GGA AAG GAC GAA ACA CCG GCT CGA CTT GAA ACC CAG AGA G-3′ and the reverse primer 5′-TGT CTC GAG GTC GAG AAT TAA AAA ACA GGA CCA TTT CTG GTG AAC-3′. Then, the GV309 vector was double digested with *Age*I and *Eco*RI, and the target gene was inserted using T4 DNA ligase (Invitrogen, USA) according to the manufacturer's guidelines. The GV309 vector contains the following elements in sequence: hU6-MCS-ubiquitin-enhanced green fluorescent protein (EGFP)-internal ribosome entry site (IRES)-

puromycin. The ligated vector was transformed into competent *Escherichia coli* DH5α cells (Invitrogen, USA). Restriction enzyme analysis and DNA sequencing were performed to identify the correct transformant. 293T cells (Shanghai Research Institute of Chinese Academy of Sciences, China) were used to generate the lentiviruses after their transduction with the expression vectors and package vectors with the use of Lipofectamine 2000 (ThermoFisher Scientific, USA). After 48 h, supernatants containing the lentiviruses GV309-miRNA-181a-EGFP-LV and GV309-neg-EGFP-LV were harvested and the remaining cells were removed by filtration with 0.45 μm filters. Ultracentrifugation (4000 × *g* at 4 °C for 10 min) was then performed to concentrate the lentiviruses.

For the assay, 5×10^3 MSCs in the logarithmic growth phase were seeded into each well of a 96-well microplate and cultured overnight. The lentiviruses were then diluted with 0.1 ml of complete MSC medium containing HitransG P (1 μg/ml, GeneChem, China) and added to transduce the seeded cells for 12 h at 37 °C. The virus-containing medium was then changed to new virus-free medium. Fluorescence microscopy (IX 53, Olympus Corporation, Japan) was used to detect GFP in the successfully transduced cells, where the percentage of GFP-positive cells was used to measure the transduction efficiency. At the multiplicity of infection of 50, the transduction efficiency of the cells was sufficient for future experiments and the virus infection did less harm to cell survival. At 2 days after transduction, the MSCs were selected with puromycin (5 μg/ml) and the surviving cells were cultured for 3 days. The miRNA-181a expression levels were determined by quantitative PCR (qPCR) with the TaqMan probe. MSCs subjected to different treatments were divided into two groups in the subsequent assays: negative control (NC) group (cells transduced with GV309-neg-EGFP-LV) and miRNA-181a-overexpressing group (cells transduced with GV309-miRNA-181a-EGFP-LV).

2.4. Exosome harvesting and identification

The conditioned medium was collected and centrifuged at 300 × *g* for 10 min, then at 3000 × *g* for 1 h, and thereafter at 10,000 × *g* for 1 h at 4 °C to remove cells and debris, and was then finally filtered through a 0.22 μm filter (Pall Life Sciences, USA). The supernatants were harvested and ultracentrifuged in centrifuge tubes (Millipore, Germany) at 50,000 × *g* for 3 h for exosome purification. The supernatant and remaining media were discarded wholly onto absorbent paper. The exosome pellets at the bottom of the tubes were resuspended in a final volume of 100 μl of PBS solution and stored at −80 °C for further research. A series of experiments were carried out for validation of the identification of the exosomal components. The protein concentration was evaluated with the bicinchoninic acid (BCA) protein assay (ThermoFisher Scientific, USA). The exosome markers CD9, CD63, thyroid-stimulating hormone (TSH), and ALG-2-interacting protein X (ALIX-101) were identified by western blot assay. Nanosized lipid bilayer vesicles were observed by transmission electron microscopy. The particle number and size assessments were conducted by nanoparticle tracking analysis with the Malvern Zetasizer Nano ZS90 instrument.

2.5. MTT proliferation assay

The effects of the exosomes on PBMC proliferation and toxicity, with or without anti-CD28 monoclonal antibody to activate the T cells in vitro, were assessed by 3-(4,5-dimethyl-2-thiazolyl)-2,5-diphenyl-2-H-tetrazolium (MTT) assay. After incubation of 5×10^3 PBMCs with exosomes at different concentrations in a 96-well plate for 72 h, 5 mg/ml MTT solution (FMS-MTT01, Fcmacs, China) was added to each well and the plates were incubated for 3 h at 37 °C. Then, the supernatant was discarded, and the crystals that had formed were dissolved with 150 μl of dimethyl sulfoxide to terminate the reaction. The optical density at a wavelength of 562 nm was measured with an Epoch microplate reader (BioTek Instrument, USA).

2.6. miRNA mimic transfection

Prior to the Treg polarization procedure, the PBMCs were transfected with the miRNA-181a precursor, negative control (NC), mimic inhibitor, or inhibitor NC, respectively, at 50 or 100 nM (Ribobio, China). The transfections were performed using Lipofectamine RNAiMAX (Invitrogen, USA) according to the manufacturer's instructions. The medium was changed at 24 h after the transfection, and the cell suspensions were re-seeded in 12-well culture plates and incubated together with new medium and Treg-stimulating antibodies and cytokines for another 48 h.

2.7. RNA extraction and quantitative reverse transcription PCR

Total RNA was extracted from PBMCs or naïve CD4+ T cells using 1 ml of TRIzol reagent (Invitrogen, USA). Then, using 0.5–1 μg of RNA as the template, reverse transcription was performed with the SuperScript RT-PCR System (P611-01, Vazyme, China) according to the manufacturer's instructions. PCR amplification was carried out on a 7500HT Fast Real-Time PCR system (Applied Biosystems, USA), with the following primers: glyceraldehyde 3-phosphate dehydrogenase (GAPDH): forward 5′-CTC AGA CAC CAT GGG GAA GGT GA-3′ and reverse 5′-ATG ATC TTG AGG CTG TTG TCA TA-3′; interleukin (IL)-1β: forward 5′-CCTCGTGCTGTCGGACCCATA-3′ and reverse 5′-CAGGCTT GTGCTCTGCTTGTGA-3′; IL-10: forward 5′-AGGGCACCCAGTCTGAGA ACA-3′ and reverse 5′-CGGCCTTGCTCTTGTTTTCAC-3′; IL-6: forward 5′-ATGAACTCCTTCTCCACAAGC-3′ and reverse 5′-CTACATTTGCCGA AGAGCCCTCAGGCTGGACTG-3′; interferon-gamma (IFN-γ): forward 5′-CGGCACAGTCATTGAAAGCCTA-3′ and reverse 5′-GTTGCTGATGGC CTGATTGTC-3′; tumor necrosis factor-alpha (TNF-α): forward 5′-ATG AAATATACAAGTTATATG-3′ and reverse 5′-TCCAGCTGCTCCTCCAC TTG-3′; U6: forward 5′-CTCGCTTCGGCAGCACA-3′ and reverse 3′-AACGCTTCACGAATTTGCGT-5′; and miRNA-181a: forward 5′-AAC ATTCAACGCTGTCGGTGAGT-3′ and reverse 3′-CTCCTTAGAATCTGTT TGCTCTCATA-5′. The relative expression levels of the specific mRNAs and miRNAs were normalized to those of U6 or GAPDH by the $2^{-\Delta\Delta Cq}$ method.

2.8. Western blot analysis

Proteins were isolated from the exosomes, cells, or tissues using RIPA buffer (KGP703, KeyGEN, China) containing protease inhibitors (S8830, Sigma, Germany) and the concentrations were determined by BCA assay (ThermoFisher Scientific, USA). The lysates were separated by sodium dodecyl sulfate-polyacrylamide gel electrophoresis and the protein levels were measured by western blot assay using an ultrasensitive ECL kit (PE0020-2, Solarbio, China) as described in our previous research [26]. GAPDH was used as the loading control. The primary antibodies used were those against CD63 (ARG55941, 1:1000, arigo Biolaboratories, USA), CD9 (PB0977, 1:1000, BOSTER), N-ALIX (ab186429, 1:1000, abcam, UK), tumor susceptibility gene 101 protein (TSG101) (ab83, 1:1000, abcam, UK), c-Fos (E-AB-70204, 1:1000, Elabscience), and GAPDH (GB11002, 1:10,000, Servicebio Inc. Laboratories, China).

2.9. Luciferase assay

A concatemer of the miRNA-181a-predicted target sequence within the c-Fos gene, and a mutant lacking complementarity with the miRNA-181a seed sequence were cloned downstream of the luciferase gene, as driven by the cytomegalovirus promoter, generating the Luc.c-Fos and Luc.Mut vectors (KeyGEN, China), respectively. Cultured HEK 293 cells were then transfected with these constructs using Lipofectamine (Invitrogen, USA) in conjunction with the miRNA-181a mimic or a

nonsense stem-loop. The cells were harvested after 48 h and their luciferase activity was assayed using the Dual-Luciferase® Reporter Assay System 10-Pack (Promega, USA). The firefly luciferase activity was normalized to the corresponding Renilla luciferase activity. Five replicates were performed.

2.10. Flow cytometric analysis

To analyze the effects of the exosomes and mimics on Treg cell induction, cell suspensions were evaluated for their expression of Treg labeled with fluorogenic antibodies. After their immunolabeling with PerCP-labeled anti-CD4 (100537, Biolegend, USA) and APC-labeled anti-CD3 (100235, Biolegend, USA) antibodies for 30 min at 4 °C, the cells were fixed and permeabilized with a permeabilization assay kit (51-9008101, BD, USA) according to the manufacturer's instructions. The permeabilized cells were washed twice with staining buffer and resuspended in 100 μl of PBS solution. They were then incubated with PE-labeled anti-Foxp3 antibody (126403, Biolegend, USA) in the dark for 30 min at 4 °C and then finally analyzed on a flow cytometric instrument (FACSAria, BD, USA) and by FlowJo software (Version 7.6.5, FlowJo, USA) to detect the ratio of Treg cells. PBMCs or näive T cells cultured without exosomes or mimics were used as the controls. All results were repeated three times.

2.11. Animal experimental protocol

The animal protocols were approved by the Institutional Ethics Committee of Nanjing Drum Tower Hospital (Approval No. 20011146) and performed in accordance with the guidelines set forth in the *Guide for the Care and Use of Laboratory Animals* published by the National Institutes of Health (8th Edition). The acute myocardial infarction model was created with C57BL/6 male mice (10 weeks old, 20–25 g), purchased (8 weeks old) from the Model Animal Research Center of Nanjing University, according to a previously reported method [26]. In brief, the mice were first anesthetized by isoflurane inhalation (1.5%–2%). Endotracheal intubation was then performed for mechanical ventilation at a tidal volume of 0.5 ml and 120 breaths/min (Alcott Biotech, China). Following chest opening at the 4th intercostal space and dissection through the intercostal muscles, a 7–0 silk suture was placed and tied around the left anterior descending coronary artery, and subsequently released after 45 min to allow for reperfusion. The animals were randomly divided into four groups: PBS, wild-type exosomes (WT-EXO), miRNA-181a-EXO, and a sham group that underwent a similar surgical procedure without aorta constriction. For the intramyocardial injection, 200 μg of exosomes suspended in PBS or the same volume of PBS only was used. Finally, the chest was closed by tightening the double purse suture. On day 3 following the myocardial I/R injury, the mice were anesthetized and placed on a warm saline bag in a shallow left lateral position, and warm coupling gel was applied to the shaved chest. Transthoracic echocardiography was performed, and the images were analyzed as described in a previous report [29]. After echocardiography, some mice were sacrificed through overdosing with a chloral hydrate solution. Blood samples were obtained by eyeball extirpation for evaluation of the inflammatory agents and Treg cell ratio. For immunohistochemical analysis of the infarct border zone, tissue slides were immunostained with anti-FoxP3 (1:100, eBioscience, USA) by using the 5-bromo-4-chloro-3-indolyl phosphate/nitroblue tetrazolium chromagen (Servicebio Inc. Laboratories, China) according to the manufacturer's protocol. The sections were co-stained with hematoxylin. The remaining mice were sacrificed on day 7 post myocardial I/R injury. The size of the infarcted myocardium was measured by the triphenyl tetrazolium chloride (TTC) and Evans blue method. In brief, the loosened ligature was left in place for subsequent occlusion prior to infusion of the Evans blue dye and then the TTC dye (Sigma, USA) at 37 °C for 15 min. The hearts were immersed in physiological saline and the left ventricles below the ligation site were then cut into 4 μm slices. After fixing with formaldehyde and staining with 1% TTC solution at 37 °C for 15 min, a camera-mounted dissecting microscope was used to photograph the tissue, and ImageJ software was used to quantify the infarct area and area at risk. The size of the heart and inflammatory cell infiltration were assessed by histological analysis with hematoxylin and eosin (H&E) staining, as detailed in our previous report [26].

2.12. Statistical analysis

All derived statistical values were expressed as a standard format mean ± standard deviation and analyzed with SPSS 17.0 (SPSS Inc., USA) or GraphPad Prism 6 (GraphPad Software, USA). Each experiment was repeated three times independently. Statistical significance was determined using Student's *t*-test for the comparison of two groups, one-way analysis of variance (ANOVA) followed by Tukey's multiple comparison test for the comparison of multiple groups, and two-way ANOVA followed by Bonferroni's multiple comparison test for comparisons between different groups over time. Differences were considered statically significant at a P value of < 0.05.

3. Results

3.1. Identification of key miRNAs and functional enrichment analysis of miRNA-181a

We conducted a bioinformatic analysis of the small RNA sequencing data obtained from a public database to determine the potential overall biological effects of the entire MSC-EXO cargo as one integrated system [30]. The miRNA expression profiles of exosomes from human bone marrow-derived MSCs were downloaded from the GEO (GSE78865) database. Because MSCs are prone to accumulating oncogenic mutations and developing decreased hematopoietic capability in the course of aging, a total of 317 (i) or 136 (ii) miRNAs were identified as having no correlation with aging or multiple myeloma-causing characteristics under the exclusion criteria. Our previous miRNA microarray profiling had shown the top 100 (iii) miRNAs in MSC-EXO [26]. By overlapping the three sets of miRNA data (i, ii, and iii) mentioned above, 25 miRNAs were taken as key small RNAs (Fig. 1A), where miRNA-181a accounted for 0.8% of the total content (Fig. 1B). To further narrow down the key miRNAs, the 25 candidate miRNAs and 1444 predicted genes were used to develop an miRNA-mRNA network. Six (miRNA-221, miRNA-222, miRNA-16b, miRNA-26a, miRNA-148, and miRNA-181a) of the top 25 candidate miRNAs obviously shared close proximity with similar gene clusters, suggesting their central role in molecular interaction and biological functions (Fig. 1C).

Because our research had found that three miRNAs (miRNA-498, miRNA-181a, and iRNA-612) were most associated with the onset and development of myocardial infarctions (Liu in our laboratory, unpublished data), we further chose miRNA-181a for a more detailed analysis. Four website tools were used to obtain potential targets of miRNA-181a in a much more precise way (Fig. 1D). It was clear that this miRNA provided substantial coverage against a host of immune-related genes. A detailed annotation of their biological processes showed that their functions were mainly enriched in the regulation of synaptic transmission, homophilic cell adhesion via plasma membrane adhesion molecules, and so forth (Fig. 1E). KEGG pathway analysis showed that the gene targets were annotated to the T cell receptor signaling pathway, ErbB signaling pathway, VEGF signaling pathway, and so forth (Fig. 1F). To gain a better understanding of how the genes, pathways, and biological processes regulated by miRNA-181a relate to one another and to obtain “communities” of proteins that work together, the target gene profiles were subjected to a protein-protein interaction network analysis, where 31 nodes (proteins) and 143 edges

(or connectivity, indicating how many links the node has to other nodes) were included (Fig. 1G) [31]. The MAPK1 node had the highest degree of 19 (18 in-degree and 1 out-degree), and c-Fos was also worth further attention (8 in-degree and 2 out-degree).

3.2. Lentivirus-mediated miRNA-181a overexpression and characterization of MSC-derived exosomes

MSCs were transduced with two different lentivirus vectors (GV309-miRNA-181a-EGFP-LV and GV309-neg-EGFP-LV), respectively. As a

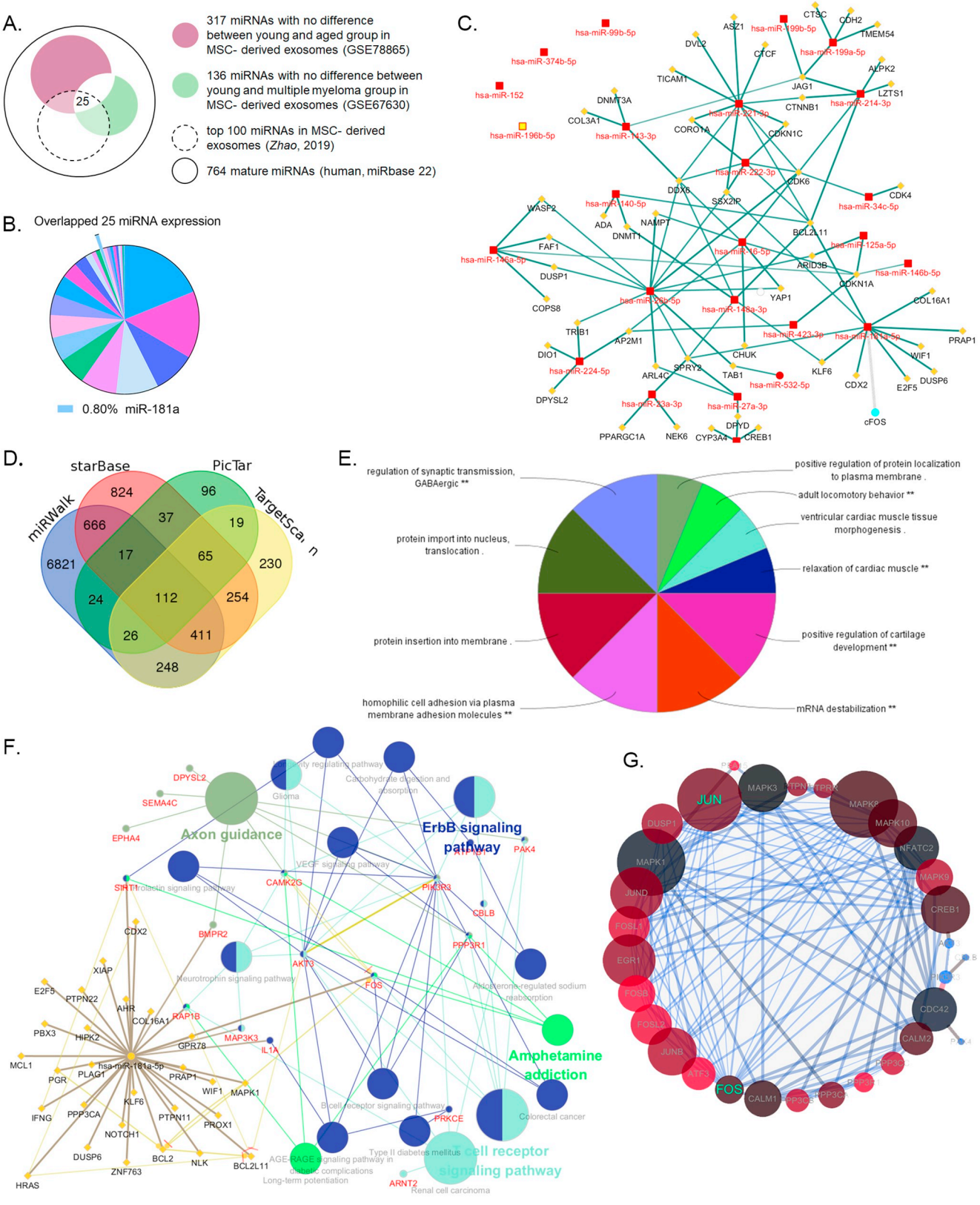

(caption on next page)

Fig. 1. MSC derived exosomes contained abundant miRNAs sharing a close proximity with similar target gene clusters. (A) 764 human mature miRNAs deposited in miRBase 22, 317 (41.5%, red circle) or 136 (17.8%, green circle) miRNAs had been determined irrelevant to aging or multiple myeloma-causing in the GEO datasets. The 25 overlapped miRNAs contained within MSC exosomes were further analyzed for processes and pathways. (B) miR-181a accounted for 0.80% of top 25 miRNAs present in MSC exosomes. (C) Enrichment map of pathways targeted by the overlapped 25 miRNAs. Nodes represent the individual genes of significantly enriched biological processes and the miRNAs which target them, connected by the edges. 6 miRNAs targeting similar gene clusters are located in close proximity to one another, (e.g., miRNA-221, miRNA-222, miRNA-16b, miRNA-26a, miRNA-148 and miRNA-181a). (D) The 112 intersection genes of has-mir-181a-5p predicted targets were obtained from miRWalk (blue oval), TargetScan (yellow oval), PicTar (green oval) and starBase (red oval) database. Charts of 112 genes enriched in (E) biological process and (F) KEGG pathway in Gene Ontology analysis using the online tool Database for Annotation Visualization and Integrated Discovery (DAVID), Funrich software and ClueGO app from Cytoscape software. (G) The gene interaction networks of 112 intersection genes putatively targeted by miR-181a. Nodes indicate proteins and edges represented as lines between genes indicate connectivity. The gene c-Fos is distinctive with higher connectivity in the network. (For interpretation of the references to colour in this figure legend, the reader is referred to the web version of this article.)

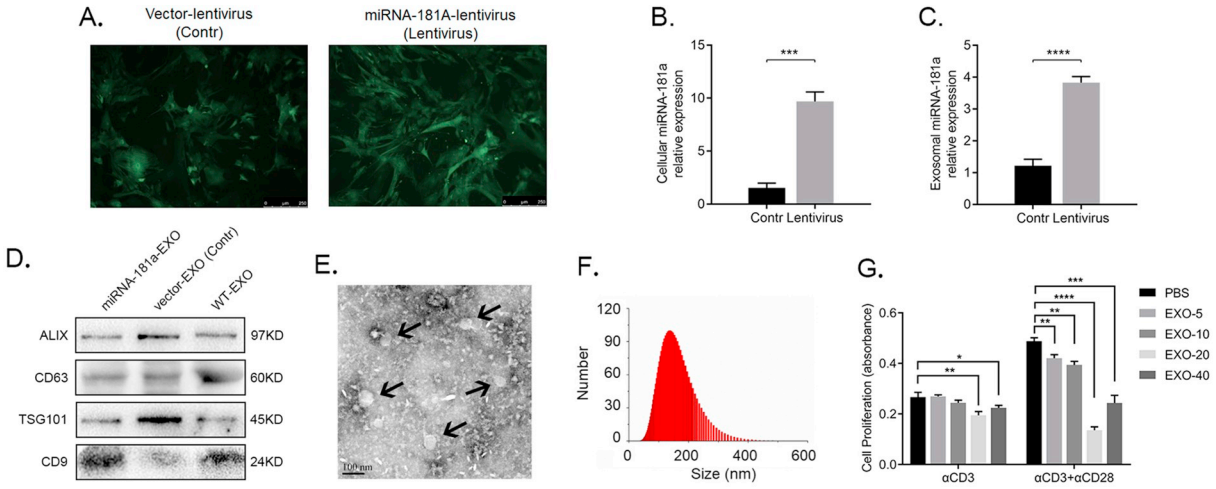

Fig. 2. Lentivirus mediated miRNA-181a over-expression in MSC-derived exosomes. (A) GFP expression in lentivirus infected MSCs recorded by fluorescence microscopy. (B, C) Real-time quantitative PCR of miRNA-181a over-expression efficiency in the vector-lentivirus and miRNA-181a-lentivirus-infected MSCs cells and exosomes ($n = 3$ each group). (D) Representative images of WB to assess the presence of ALIX, CD9, CD63 and TSG101 in miRNA-181a-lentivirus infected exosomes. (E) Transmission electron micrograph of MSC-derived exosomes. (F) Nanoparticle trafficking analyzed the diameters and concentration of exosomes. (G). MTT assay showed that cell proliferation was significantly reduced in MSCs after co-stimulated with anti-CD28 and anti-CD3. ($n = 6$ each group). * $P < 0.05$, ** $P < 0.005$, *** $P < 0.0005$, **** $P < 0.0001$.

result, ≥95% of the transduced MSCs expressed GFP after 72 h, as observed under a fluorescence microscope (Fig. 2A, Supplementary Fig. 1), indicating the successful construction of a highly efficient and stable vector. Both the cellular and exosomal miRNA-181a post-transcriptional levels in the MSCs transduced with the miRNA-181a-carrying lentivirus were significantly increased relative to those of MSCs transduced with the control vector (Fig. 2B & C), as determined by qPCR analysis. These data suggested that the exosomal expression of miRNA-181a was efficiently upregulated following GV309-miRNA-181a-EGFP-LV transduction. Exosomes obtained from the GV309-miRNA-181a-EGFP-LV-transduced MSCs exhibited a typical cup-shaped morphology (Fig. 2E). All were positive for the exosomal surface markers CD9, CD63, ALIX, and TSG101 (Fig. 2D). We also examined the size of the exosomes derived from the GV309-miRNA-181a-EGFP-LV-transduced MSCs. Dynamic light scattering analysis showed that the size distribution profile was physically homogeneous, with a peak diameter of 87.6 nm (Fig. 2F), indicating their cytoplasmic origin.

3.3. Effects of miRNA-181a on the inflammatory response and Treg polarization in PBMCs

To activate T-cell proliferation, PBMCs were plated in 12-well culture plates precoated overnight at 4 °C with 0.5 μg/ml anti-CD3 antibody diluted in PBS (300306, BioLegend, USA). To promote Treg polarization, lineage-driving antibodies and cytokines, including 0.2 μg/ml anti-CD28 antibody (302913, BioLegend, USA), 1 ng/ml TGF-β (PCK091, Procell, China), and 100 U/ml IL-2 (ELS-CYT024, Elsbio, China), were added to the PBMC complete medium as previously described [32,33]. However, because conditional knockout mice with the Treg-specific deletion of CD28 have been proven to have normal numbers of Treg cells [34], many researchers have chosen a single cytokine (anti-CD3) as a guardian of Treg cell survival, with satisfactory experimental results (Fig. 3) [35,36]. In this present study, PBMC proliferation was detected by MTT after 3 days of stimulation. Compared with those pre-stimulated by a single cytokine (anti-CD3), PBMCs subjected to two-hit pre-stimulation (anti-CD28 and anti-CD3) showed significant proliferation inhibition, and the effect was more obvious with increases in the exosome concentration. However, these effects were not dose dependent in the PBMCs exposed to anti-CD3 pre-treatment only (Fig. 2G). Therefore, in this study, we chose anti-CD3 + 40 μg/l exosomes as the optimal culture conditions in vitro.

With regard to inflammatory cell infiltration, the miRNA-181a mimics downregulated the pro-inflammatory cytokines TNF-α and IL-6 and significantly increased the expression of the anti-inflammatory cytokine IL-10 in the PBMCs. The same trend was observed for the PBMCs co-cultured with exosomes derived from lentivirus-transduced MSCs but at a slightly lower degree. No significant changes were observed in the PBMCs cultured with PBS solution or with untreated exosomes (Fig. 3A). With regard to Treg polarization, the miRNA-181a mimic was able to induce the formation of T cells with a Treg phenotype (CD4+ CD25+ Foxp3). We were also able to observe remarkable differences in Treg induction when the PBMCs were co-cultured with either WT-EXO or miRNA-181a-EXO compared with their PBS-treated counterparts (Fig. 3B). Because the mechanism of this phenomenon has been rarely studied, we next focused on the c-Fos protein and the hypothesis that miRNA-181a might initiate Treg differentiation by targeting c-Fos. To test this hypothesis, antibodies and cytokines for Treg polarization were added to the PBMC complete medium before addition

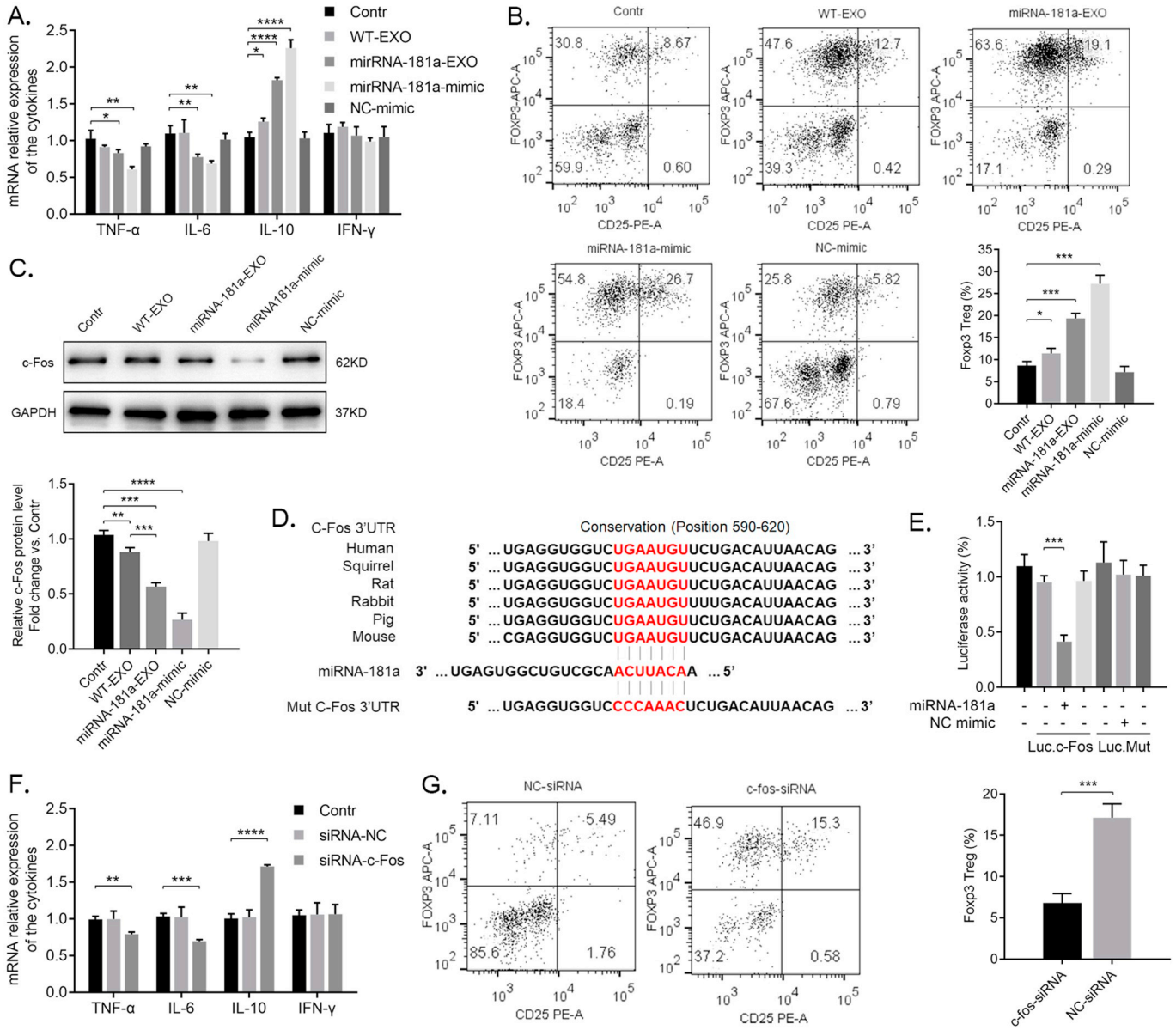

Fig. 3. miRNA-181a over-expression inhibited the immune inflammatory response and raised Treg polarization by targeting c-Fos gene in PBMCs. (A) Expression of the cytokines in anti-CD3 pre-stimulated PBMCs analyzed by Real-time qPCR (n = 3 each group). (B) FACS assay of Treg population measured by CD4 + CD25 + FOXP3 after transfecting with miRNA-181a mimic, MSC exosomes or miRNA-181a overexpressed exosomes, expressed as a percentage of the total number of CD4 cells (n = 3 each group). (C) Immunoblot analyses of c-Fos transfected with miRNA-181a mimic, MSC exosomes or miRNA-181a overexpressed exosomes (n = 3 each group). (D) Luciferase reporter constructs containing the wild-type or mutated 3′-UTR of mouse c-Fos mRNA. The sequence in red indicates the predicted binding site for miRNA-181a, aligning with miRNA-181a seed sequence. (E) Relative luciferase activity normalized to vector (n = 3 each group). (F) Expression of the cytokines in anti-CD3 pre-stimulated PBMCs analyzed by real-time qPCR (n = 3 each group). (G) FACS assay of Treg population measured by CD4 + CD25 + FOXP3 after transfecting with siRNA, expressed as a percentage of the total number of CD4 cells (n = 3 each group). * $P < 0.05$, ** $P < 0.005$, **** $P < 0.0001$.

of the miRNA-181a mimic. As determined by western blot analysis, the miRNA-181a mimic and miRNA-181a-EXO significantly inhibited the c-Fos protein levels in the cells (Fig. 3C). These results confirmed the conclusion drawn by the computational approaches used to identify the miRNA-mRNA interaction between miRNA-181a and the c-Fos protein (Fig. 1G). According to the computational analysis, miRNA-181a was predicted to be incorporated into an RNA-induced silencing complex that binds with a target mRNA and conserved binding sites in the 3′-untranslated region (UTR) of the c-Fos mRNA across multiple species (Fig. 3D). A construct containing the 3′-UTR of the c-Fos mRNA or the sequence with the mutant seed region was co-transfected together with the miRNA-181a mimic or a scrambling miRNA. As we had predicted, the miRNA-181a mimic specifically reduced the Luci-WT-3′-UTR luciferase activity, whereas no inhibition was evident with the mutant construct (Fig. 3E). The luciferase reporter gene assay further confirmed that miRNA-181a bound directly to the 3′-UTR of c-Fos on the molecular level. We further explored the relationship between c-Fos and changes in local inflammation through siRNA-mediated gene silencing. c-Fos-siRNA downregulated TNF-α and IL-6 and upregulated both IL-10 and the proportion of Treg cells (Fig. 3F & G). These results verified that the effects of miRNA-181a on the inflammatory response and Treg polarization were through the targeting of c-Fos.

3.4. Effect of miRNA-181a overexpression in MSC-derived exosomes on ischemic damage in vivo

To investigate the role of exogenous miRNA-181a-EXO in adult myocytes, we subjected C57BL/6 mice to 45 min of ischemia followed

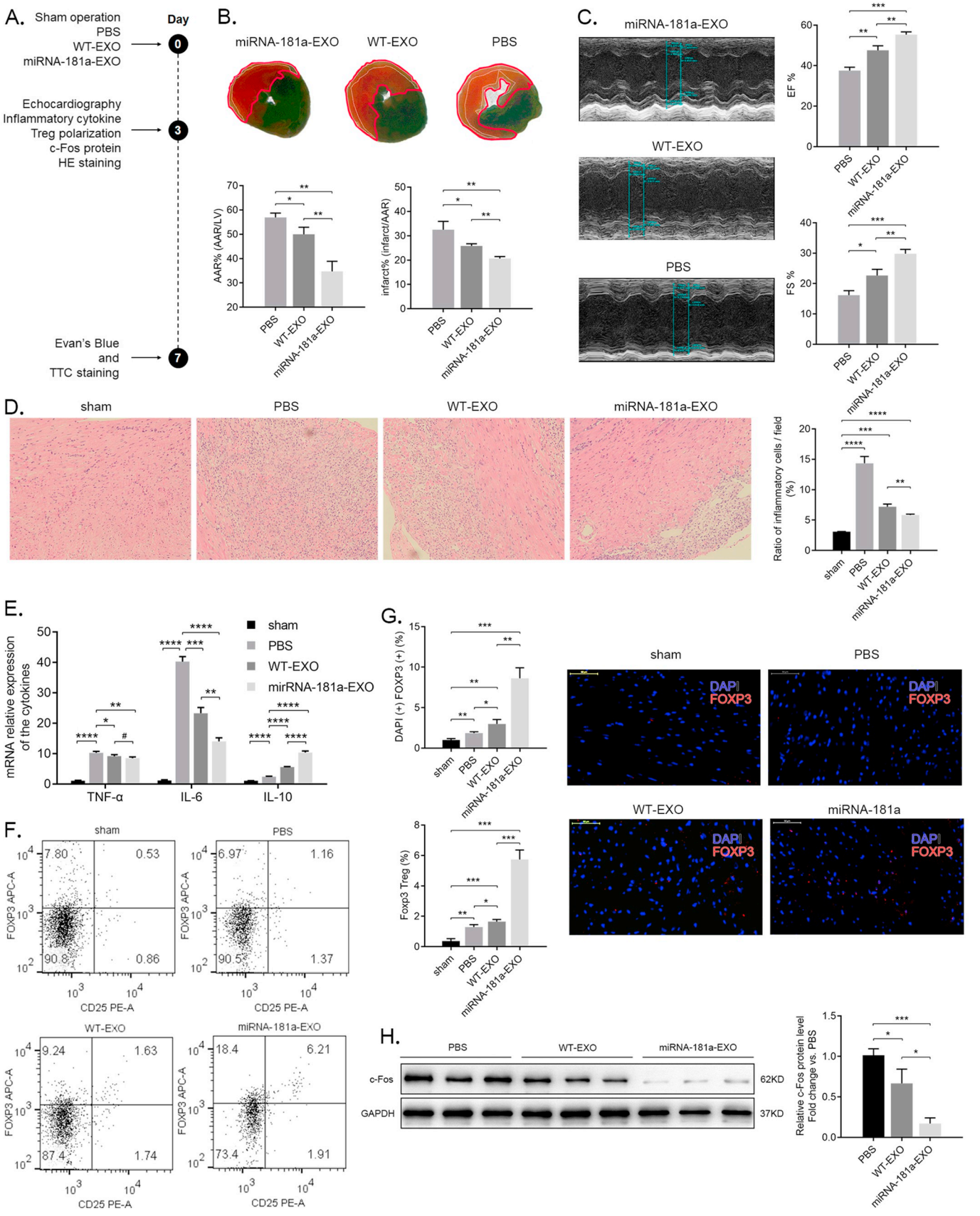

(caption on next page)

Fig. 4. Over-expressing miRNA-181a in MSC exosomes retarded ischemic damage in vivo. (A) In vivo experimental process flow chart. (B) Representative images and qualification of Evans Blue and TTC-stained hearts isolated from mice 7 days following treatment with MSC exosomes or miRNA-181a overexpressed exosomes. Area-at-risk (AAR, red line) and infarct size (IS, white dotted line) ($n = 3$ each group). (C) Representative echocardiograms of and EF% and FS% measurement results 3 days following myocardial I/R injury ($n = 5$ each group). (D) HE staining and quantification of inflammatory cell infiltration (%) within the ischemic myocardium 3 days following myocardial I/R injury ($n = 5$ each group). (E) Expression of the cytokines in mouse heart tissues analyzed by real-time qPCR ($n = 4$ each group). (F) FACS assay of Treg population measured by CD4 + CD25 + FOXP3 after intramyocardial injection with MSC exosomes or miRNA-181a overexpressed exosomes, expressed as a percentage of the total number of CD4 cells ($n = 4$ each group). (G) Representative images and quantification of FoxP3 (+) Treg cells by immunofluorescence ($n = 3$ each group). (H) Immunoblot analyses of c-Fos transplanted with PBS, MSC exosomes or miRNA-181a overexpressed exosomes ($n = 3$ each group). * $P < 0.05$, ** $P < 0.005$, **** $P < 0.0001$. (For interpretation of the references to colour in this figure legend, the reader is referred to the web version of this article.)

by reperfusion (I/R) or a sham operation without aortic ligation. Then, the I/R injury-modeling mice were randomly divided into the PBS control group, EXO-treated group, and miRNA-181a-EXO-treated group for intramyocardial injection with the respective treatments (Fig. 4A). On day 7 post treatment, the cardiac function and physical parameters were assessed by echocardiography. A higher ejection fraction (EF (%)) and fractional shortening (%) were detected in the miRNA-181a-EXO-treated group, in addition to a slight EF (%) improvement in the EXO-treated group (Fig. 4B). Evans blue and TTC staining revealed that the infarct area was visible in all three groups except the sham group, and the percentages of the infarct area and the area at risk in the miRNA-181a-EXO-treated group were significantly lower than those in the PBS control group and EXO-treated group (Fig. 4C).

To determine how the changes in the infarct area and cardiac function were related to the local inflammatory reaction, we focused mainly on the effect of inflammatory mediator secretion and Treg cell polarization at day 3 post exosome treatment. H&E staining of the heart revealed reduced inflammatory cell infiltration in the miRNA-181a-EXO-treated group (Fig. 4D), indicating that the miRNA-181a delivered by MSC-EXO could modulate the level of inflammation following myocardial I/R injury. Samples of the mouse heart tissues were ground and detected by RT-qPCR. MSC-EXO likely slowed down the inflammatory damage by intervening in the expression of the inflammatory factors IL-6, TNF-α, and IL-10. A significant promotion of the anti-inflammatory cytokine IL-10 and a robust decrease of the pro-inflammatory cytokines IL-6 and TNF-α were detected in the miRNA-181a-EXO-treated group (Fig. 4E). We then focused on the key inflammatory regulator of Treg cells. Flow cytometric (Fig. 4F) and immunofluorescence analyses (Fig. 4G) showed that the ratio of CD25 + Foxp3 Treg cells to the total CD4 + cells was higher in the WT-EXO-treated group than in the sham operation group or PBS control group, whereas significantly more Treg cells were counted in the miRNA-181a-EXO-treated group. To investigate the molecular mechanism behind this improvement of microinflammation, we evaluated the expression level of proteins downstream of miRNA-181a in the cardiac tissues. The western blot analysis showed that c-Fos was significantly inhibited in the miRNA-181a-EXO-treated group. Taken together, these results indicated that miRNA-181a delivery by MSC-EXO suppressed the inflammatory response and promoted Treg cell development through a mechanism that may involve c-Fos inhibition.

4. Discussion

MiRBase (http://www.mirbase.org/) is a database of published miRNA sequences and annotations, with > 35,828 mature miRNAs from over 223 species, and the list is still growing [37]. This incremental body of data has guaranteed researchers the opportunity to examine the internal associations of miRNA signatures with interaction networks in large cohorts and functional studies. In this study, we demonstrated that MSC-EXO containing miRNA-221, miRNA-222, miRNA-16b, miRNA-26a, miRNA-148, and miRNA-181a shared crossed biological functions with crossed downstream gene clusters. miRNA-181a, the focus of this research, targeted a network of inflammation-related genes, suggesting its central role in immune regulation. We discover that the lentivirus-mediated overexpression of miRNA-181a in MSCs could also lead to an obvious upregulation of miRNA-181a in exosomes. Our study first revealed that miRNA-181a delivery by MSC-EXO exerted a protective role during myocardial I/R injury progression. Moreover, we also determined the seldom-reported proteins downstream of miRNA-181a using computational approaches, and fully validated the results using the dual luciferase reporter system.

Acute myocardial infarction accounts for a large proportion of cardiac-related deaths among humans. With the establishment of chest pain centers worldwide, increasingly more patients with intense chest pain have been able to undergo coronary artery revascularization through the “green channel.” However, a fair number of patients are still faced with the deterioration of their cardiac function after emergency percutaneous coronary intervention. Myocardial I/R injury, a process closely linked with an excessive inflammatory response, has been proven to be the major cause of cardiac deterioration and death [38]. Following myocardial I/R injury, a variety of damage-associated molecules are released from the necrotic cardiac tissue to resident cells, thereby inducing an inflammatory cascade within the heart. Thus, stem cell-based therapy and Treg cell transplantation have become two attractive and promising approaches for the treatment of I/R injury, mainly because of their therapeutic effects in inhibiting excessive inflammation [7,39]. However, the use of exogenous Treg cells is often limited by the shortages of donors and cell induction. Therefore, there is an urgent need to find a practical way to activate Treg cells early after myocardial infarction. Interestingly, MSCs have been found to secrete exosomes, which are considered as vital mediators of cellular communication and may regulate various physiological and pathological processes by transferring membrane protein, mRNAs, and miRNAs to recipient cells. On the bases of the morphological characteristics and carrier potential of the exosomes, we innovatively developed an effective approach to specifically deliver miRNA-181a to mouse heart tissue through MSC-EXO intramyocardial injection, which could enhance the original role of the MSC-EXO in stimulating the secretion of IL-10 by mononuclear cells and inducing the development of Treg cells.

Recent research studies have linked miRNA-181a to cardiovascular inflammatory infiltrates and immune cell imbalance in various cell types. The lymphatic vasculature acts as a pathway for immune cells during inflammation. In cardiac lymphatic vascular endothelial cells (LECs), a higher expression of miRNA-181a may help to prevent the formation of a high LEC identity by silencing the expression of the homeobox transcription factor prospero homeobox 1 (Prox1) [40]. In vascular smooth muscle cells, miR181a overexpression inhibited the adhesion of the cells to collagen by inhibiting angiotensin II-induced osteopontin expression [41]. In mature T cells, miRNA-181a could inhibit positive selection and T-cell maturation by downregulating B-cell lymphoma 2, CD69, and the T-cell receptor [42]. Geoffrey et al. found that the miRNA-181 family contained in cardiosphere cell-derived exosomes served as a strong candidate for macrophage polarization [43]. In DCs, the luciferase assay confirmed that ox-LDL-induced inflammation could be repressed by miRNA-181a, partly as a result of the targeting of the 3′-UTR of the c-Fos protein [44]. In this present study, we mainly probed the cardioprotective effect of miRNA-181a and its downstream c-Fos protein on monocytes.

c-Fos is considered a key immunoactivator that contributes to DC-related immune functions from all links and processions. DCs initiate

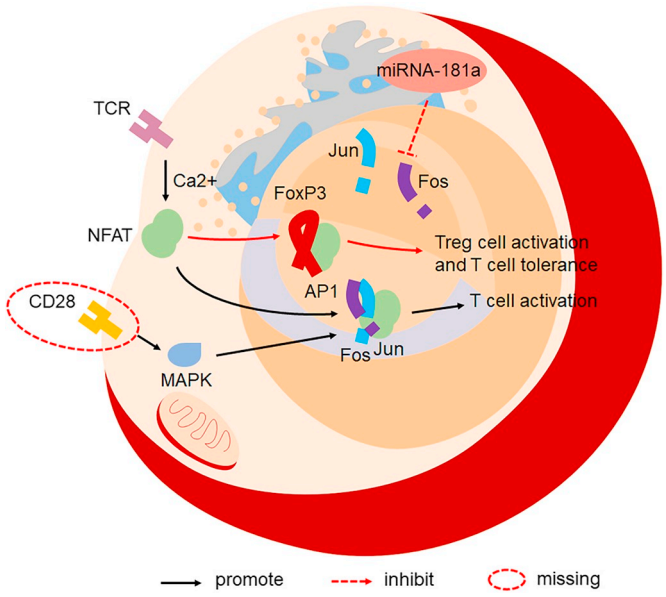

Fig. 5. Possible mechanism through which Foxp3 promotes Treg cell development, by competing with activator protein 1 (AP1) for binding with n*uclear factor of activated T cells (*NFAT). c-Fos, a main component of AP1, is downregulated by miRNA-181a, leading to T-cell tolerance and Treg cell development.

the immune response by migrating from far-off inflammatory sites to the lymph nodes and presenting antigens to the antigen-specific naïve T cells. Prostaglandin E2 could induce DC migration briefly through the EP2/EP4 → cAMP → protein kinase A/PI3K → ERK → c-Fos pathway, and reduced the protein expression of c-Fos, leading to the attenuation of DC migration [45]. One study found that when DCs reached the peripheral immune organs, the brief contact between the DCs and T cells immediately elevated c-Fos expression and activated the rapid encounter of the T cells with an antigen-bearing stimulation [46]. Moreover, c-Fos is a component of the transcription factor activator protein 1 (AP1). Previous studies have shown that cooperative binding of Foxp3 with nuclear factor of activated T cells (NFAT) is required for Treg cell stimulation. AP1 is similarly able to bind with NFAT on the very same binding site, leaving the unbound Foxp3 unable to exert its biological function [47]. The lentivirus-mediated overexpression of AP1 in naïve T cells massively repressed the formation of T cells with the Treg phenotype [48]. We reasonably inferred that the downregulation of c-Fos expression by miRNA-181a could increase Treg polarization in human peripheral blood mononuclear cells (Fig. 5). In this study, we demonstrated that miRNA-181a overexpression significantly inhibited the inflammatory response and raised the Treg cell ratio by targeting c-Fos, a crucial inflammatory transcription factor. Thus, miRNA-181a delivery by MSC-EXO combined the immune suppressive effect of miRNA-181a and the cell targeting capability of MSC-EXO, eventually exerting a stronger therapeutic effect on myocardial I/R injury.

We acknowledge that this study had several limitations that could be improved. In future studies, the PBMCs should be replaced by human CD4+ naïve T cells for a more convincing result. The cause-and-effect relationship between cytokine secretion and Treg development should be described through a rigorous experiment. Overexpression and gene-knockout tests should be performed to evaluate the internal links between miRNA-181a and c-Fos under careful and deliberate consideration. In addition, considering that miRNA-181a was also found to increase Treg cell formation as a direct target of Smad7, an inhibitor of TGF-β signaling [15], it is clear that exosomes and their miRNAs have protean effects. Picking a single candidate as the cause of the effects shown may oversimplify the actual biology. Further studies should focus on the differences in expression levels of the downstream molecules mentioned above.

5. Conclusion

Our results indicate that miRNA-181a may inhibit the inflammatory response and raise the Treg cell ratio through inhibition of the c-Fos protein. miRNA-181a delivery by MSC-EXO combined the immune suppressive effect of miRNA-181a and the cell targeting capability of MSC-EXO to exert a stronger therapeutic effect on myocardial I/R injury. Exosomes could serve as a potential tool for the specific delivery of small RNAs in vivo.

Abbreviations

Treg	T regulation cell
MSC	mesenchymal stem cell
CDC	cardiosphere-derived cell
PBMC	peripheral blood mononuclear cell
VSMC	vascular smooth muscle cell
AMI	acute myocardial infarction
PCI	percutaneous coronary intervention
I/R	ischemia followed by reperfusion
EXO	exosome
EV	extracellular vehicle
CVD	cardiovascular disease
DC	dendritic cell
GEO	Gene Expression Omnibus
KEGG	Kyoto Encyclopedia of Genes and Genomes
DEG	differential expressed gene
LV	lentivirus
DLS	dynamic light scattering
UTR	untranslated regions
LAD	left anterior descending coronary artery
EF	ejection fraction
FS	fractional shortening
NC	negative control

Author contributions

Wei Z.L., and Qiao S.H., designed the study. Wei Z.L., wrote this manuscript and Qiao S.H. finished experiments. Xu B. gave the structure of this dissertation. Wei Z.L., and Liu Y.H., performed the bioinformatics analysis. Li Q.L., oversaw language edit. All authors read and approved the final manuscript.

Funding

This work was supported by grants from the Natural Science Foundation of China (81700392), the Funds for Jiangsu Provincial Key Medical Discipline (ZDXKB2016013), the Key Projects of Science and Technology of Jiangsu Province (BE2016607), Natural Science Foundation of Jiangsu Province – Youth Fund Project (BK20150106), the Funds for Distinguished Young Scientists in Nanjing (JQX15002), the Programs of the Science Foundation in Nanjing (QRX17113, YKK17085 and YKK17095), the Postgraduate Research & Practice Innovation Program of Jiangsu Province (Grant #. KYCX18_1462), and the Nanjing Health Youth Talent Training Project in 13th Five-Year (grant no. QRX17113).

Declaration of Competing Interest

The authors declare no competing financial interests regarding the publication of the present study.

Acknowledgments

The authors would like to thank those previous researchers who updated their data onto the databases employed in the present study.

The microarray data of GSE78865, GSE26731, GSE49823 and GSE28858 can be obtained from NCBI-GEO online database (https://www.ncbi.nlm.nih.gov/geo/query/acc.cgi).

Appendix A. Supplementary data

Supplementary materials can be found at www.mdpi.com/xxx/s1. Supplementary data to this article can be found online at doi: https://doi.org/10.1016/j.lfs.2019.116632.

References

[1] J.N. Cohn, R. Ferrari, N. Sharpe, Cardiac remodeling—concepts and clinical implications: a consensus paper from an international forum on cardiac remodeling. Behalf of an International Forum on Cardiac Remodeling, J. Am. Coll. Cardiol. 35 (3) (2000) 569–582.

[2] D.J. Hausenloy, D.M. Yellon, Myocardial ischemia-reperfusion injury: a neglected therapeutic target, J. Clin. Invest. 123 (1) (2013) 92–100.

[3] Z. Wang, J. Yu, J. Wu, F. Qi, H. Wang, Z. Wang, Z. Xu, Scutellarin protects cardiomyocyte ischemia-reperfusion injury by reducing apoptosis and oxidative stress, Life Sci. 157 (2016) 200–207.

[4] Y.Y. Cheng, D. Luo, Z. Xia, H.F. Tse, X. Li, J. Rong, In vivo cardioprotective effects and pharmacokinetic profile of N-propyl caffeamide against ischemia reperfusion injury, Arch. Immunol. Ther. Exp. 65 (2) (2017) 145–156.

[5] D.M. Richards, M. Delacher, Y. Goldfarb, D. Kagebein, A.C. Hofer, J. Abramson, M. Feuerer, Treg cell differentiation: from thymus to peripheral tissue, Prog. Mol. Biol. Transl. Sci. 136 (2015) 175–205.

[6] Y.P. Wang, Y. Xie, H. Ma, S.A. Su, Y.D. Wang, J.A. Wang, M.X. Xiang, Regulatory T lymphocytes in myocardial infarction: a promising new therapeutic target, Int. J. Cardiol. 203 (2016) 923–928.

[7] T.T. Tang, J. Yuan, Z.F. Zhu, W.C. Zhang, H. Xiao, N. Xia, X.X. Yan, S.F. Nie, J. Liu, S.F. Zhou, J.J. Li, R. Yao, M.Y. Liao, X. Tu, Y.H. Liao, X. Cheng, Regulatory T cells ameliorate cardiac remodeling after myocardial infarction, Basic Res. Cardiol. 107 (1) (2012) 232.

[8] N.G. Frangogiannis, Regulation of the inflammatory response in cardiac repair, Circ. Res. 110 (1) (2012) 159–173.

[9] D. Goltz, K. Hittetiya, H. Gevensleben, J. Kirfel, L. Diehl, R. Meyer, R. Buttner, Loss of the LIM-only protein Fhl2 impairs inflammatory reaction and scar formation after cardiac ischemia leading to better hemodynamic performance, Life Sci. 151 (2016) 348–358.

[10] F. Bagheri, V. Khori, A.M. Alizadeh, S. Khalighfard, S. Khodayari, H. Khodayari, Reactive oxygen species-mediated cardiac-reperfusion injury: mechanisms and therapies, Life Sci. 165 (2016) 43–55.

[11] C.Z. Chen, L. Li, H.F. Lodish, D.P. Bartel, MicroRNAs modulate hematopoietic lineage differentiation, Science (New York, N.Y.) 303 (5654) (2004) 83–86.

[12] S. Dolati, F. Marofi, Z. Babaloo, L. Aghebati-Maleki, L. Roshangar, M. Ahmadi, R. Rikhtegar, M. Yousefi, Dysregulated network of miRNAs involved in the pathogenesis of multiple sclerosis, Biomed. Pharmacother. 104 (2018) 280–290.

[13] S. Ultimo, G. Zauli, A.M. Martelli, M. Vitale, J.A. Mccubrey, S. Capitani, L.M.J.O. Neri, Cardiovascular Disease-Related miRNAs Expression: Potential Role as Biomarkers and Effects of Training Exercise, vol. 9, (2018), p. 17238 (24).

[14] F. Noorbakhsh, K.K. Ellestad, F. Maingat, K.G. Warren, M.H. Han, L. Steinman, G.B. Baker, C. Power, Impaired neurosteroid synthesis in multiple sclerosis, Brain J. Neurol. 134 (Pt 9) (2011) 2703–2721.

[15] S. Ghorbani, F. Talebi, W.F. Chan, F. Masoumi, M. Vojgani, C. Power, F. Noorbakhsh, MicroRNA-181 variants regulate T cell phenotype in the context of autoimmune neuroinflammation, Front. Immunol. 8 (2017) 758.

[16] S. Ghorbani, F. Talebi, S. Ghasemi, A. Jahanbazi Jahan Abad, M. Vojgani, F. Noorbakhsh, miR-181 interacts with signaling adaptor molecule DENN/MADD and enhances TNF-induced cell death, PLoS One 12 (3) (2017) e0174368.

[17] M. Eusebio, P. Kuna, L. Kraszula, M. Kupczyk, M. Pietruczuk, Allergy-related changes in levels of CD8 + CD25 + FoxP3(bright) Treg cells and FoxP3 mRNA expression in peripheral blood: the role of IL-10 or TGF-beta, J. Biol. Regul. Homeost. Agents 28 (3) (2014) 461–470.

[18] P. Lu, Y. Cao, M. Wang, P. Zheng, J. Hou, C. Zhu, J. Hu, Mature dendritic cells cause Th17/Treg imbalance by secreting TGF-beta1 and IL-6 in the pathogenesis of experimental autoimmune encephalomyelitis, Central-European journal of immunology 41 (2) (2016) 143–152.

[19] J.N. Li, J.X. Li, H.L. Huang, X.L. Zhu, H. Ding, C.F. Huang, J. Lin, J.G. Huang, Z.C. Wu, M. Ashraf, Y.G. Wang, X.K. Li, S.Y. Zheng, J.M. Chen, H.M. Guo, J. Zhuang, P. Zhu, Influence of sirolimus-induced TGF-beta secretion on mouse Treg cell proliferation, Genet. Mol. Res. 14 (4) (2015) 18569–18579.

[20] T. Aiso, S. Takigami, A. Yamaki, H. Ohnishi, Degradation of serum microRNAs during transient storage of serum samples at 4, Ann. Clin. Biochem. 55 (1) (2018) 178–180.

[21] E. Ban, T.H. Kwon, A. Kim, Delivery of therapeutic miRNA using polymer-based formulation, Drug delivery and translational research (2019).

[22] G. Kibria, E.K. Ramos, Y. Wan, D.R. Gius, H. Liu, Exosomes as a drug delivery system in cancer therapy: potential and challenges, Mol. Pharm. 15 (9) (2018) 3625–3633.

[23] K. English, B.P. Mahon, Allogeneic mesenchymal stem cells: agents of immune modulation, J. Cell. Biochem. 112 (8) (2011) 1963–1968.

[24] K. Akiyama, C. Chen, D. Wang, X. Xu, C. Qu, T. Yamaza, T. Cai, W. Chen, L. Sun, S. Shi, Mesenchymal-stem-cell-induced immunoregulation involves FAS-ligand-/FAS-mediated T cell apoptosis, Cell Stem Cell 10 (5) (2012) 544–555.

[25] R. Kishore, M. Khan, More than tiny sacks: stem cell exosomes as cell-free modality for cardiac repair, Circ. Res. 118 (2) (2016) 330–343.

[26] J. Zhao, X. Li, J. Hu, F. Chen, S. Qiao, X. Sun, L. Gao, J. Xie, B. Xu, Mesenchymal stromal cell-derived exosomes attenuate myocardial ischemia-reperfusion injury through miR-182-regulated macrophage polarization, Cardiovasc. Res. 115 (7) (2019) 1205–1216, https://doi.org/10.1093/cvr/cvz040.

[27] X. Sun, A. Shan, Z. Wei, B. Xu, Intravenous mesenchymal stem cell-derived exosomes ameliorate myocardial inflammation in the dilated cardiomyopathy, Biochem. Biophys. Res. Commun. 503 (4) (2018) 2611–2618.

[28] S. Davis, PS. Meltzer, GEOquery: a bridge between the Gene Expression Omnibus (GEO) and BioConductor, Bioinformatics 23 (14) (2007) 1846–1847.

[29] D. Sayed, M. He, C. Hong, S. Gao, S. Rane, Z. Yang, M. Abdellatif, MicroRNA-21 is a downstream effector of AKT that mediates its antiapoptotic effects via suppression of Fas ligand, J. Biol. Chem. 285 (26) (2010) 20281–20290.

[30] Z. Wei, Y. Liu, S. Qiao, X. Li, Q. Li, J. Zhao, J. Hu, Z. Wei, A. Shan, X. Sun, B. Xu, Identification of the potential therapeutic target gene UBE2C in human hepatocellular carcinoma: an investigation based on GEO and TCGA databases, Oncol. Lett. 17 (6) (2019) 5409–5418.

[31] A.L. Barabasi, Z.N. Oltvai, Network biology: understanding the cell's functional organization, Nat. Rev. Genet. 5 (2) (2004) 101–113.

[32] A. Schmidt, S. Elias, R.N. Joshi, J. Tegner, In vitro differentiation of human CD4 + FOXP3 + induced regulatory T cells (iTregs) from naive CD4 + T cells using a TGF-beta-containing protocol, J. Vis. Exp. 118 (2016).

[33] S.C. Warth, V. Heissmeyer, Adenoviral transduction of naive CD4 T cells to study Treg differentiation, J. Vis. Exp. (78) (2013).

[34] R. Zhang, A. Huynh, G. Whitcher, J. Chang, J.S. Maltzman, L.A. Turka, An obligate cell-intrinsic function for CD28 in Tregs, J. Clin. Invest. 123 (2) (2013) 580–593.

[35] L. Kilpinen, U. Impola, L. Sankkila, I. Ritamo, M. Aatonen, S. Kilpinen, J. Tuimala, L. Valmu, J. Levijoki, P. Finckenberg, P. Siljander, E. Kankuri, E. Mervaala, S. Laitinen, Extracellular membrane vesicles from umbilical cord blood-derived MSC protect against ischemic acute kidney injury, a feature that is lost after inflammatory conditioning, J Extracell Vesicles (2) (2013).

[36] C. Weber, S. Meiler, Y. Doring, M. Koch, M. Drechsler, R.T. Megens, Z. Rowinska, K. Bidzhekov, C. Fecher, E. Ribechini, M.A. van Zandvoort, C.J. Binder, I. Jelinek, M. Hristov, L. Boon, S. Jung, T. Korn, M.B. Lutz, I. Forster, M. Zenke, T. Hieronymus, T. Junt, A. Zernecke, CCL17-expressing dendritic cells drive atherosclerosis by restraining regulatory T cell homeostasis in mice, J. Clin. Invest. 121 (7) (2011) 2898–2910.

[37] B. Fan, A.O.Y. Luk, J.C.N. Chan, R.C.W. Ma, MicroRNA and diabetic complications: a clinical perspective, Antioxid. Redox Signal. 29 (11) (2017) 1041–1063, https://doi.org/10.1089/ars.2017.7318.

[38] R. Fernandez-Jimenez, J. Garcia-Prieto, J. Sanchez-Gonzalez, J. Aguero, G.J. Lopez-Martin, C. Galan-Arriola, A. Molina-Iracheta, R. Doohan, V. Fuster, B. Ibanez, Pathophysiology underlying the bimodal edema phenomenon after myocardial ischemia/reperfusion, J. Am. Coll. Cardiol. 66 (7) (2015) 816–828.

[39] X. Cui, Z. He, Z. Liang, Z. Chen, H. Wang, J. Zhang, Exosomes from adipose-derived mesenchymal stem cells protect the myocardium against ischemia/reperfusion injury through Wnt/beta-catenin signaling pathway, J. Cardiovasc. Pharmacol. 70 (4) (2017) 225–231.

[40] J. Kazenwadel, M.Z. Michael, N.L. Harvey, Prox1 expression is negatively regulated by miR-181 in endothelial cells, Blood 116 (13) (2010) 2395–2401.

[41] E.W. Remus, A.N. Lyle, D. Weiss, N. Landazuri, M. Weber, C. Searles, W.R. Taylor, miR181a protects against angiotensin II-induced osteopontin expression in vascular smooth muscle cells, Atherosclerosis 228 (1) (2013) 168–174.

[42] J.R. Neilson, G.X. Zheng, C.B. Burge, P.A. Sharp, Dynamic regulation of miRNA expression in ordered stages of cellular development, Genes Dev. 21 (5) (2007) 578–589.

[43] G. de Couto, R. Gallet, L. Cambier, E. Jaghatspanyan, N. Makkar, J.F. Dawkins, B.P. Berman, E. Marbán, Exosomal microRNA transfer into macrophages mediates cellular postconditioning clinical perspective, Circulation 136 (2) (2017) 200–214.

[44] C. Wu, Y. Gong, J. Yuan, W. Zhang, G. Zhao, H. Li, A. Sun, KaiHu, Y. Zou, J. Ge, microRNA-181a represses ox-LDL-stimulated inflammatory response in dendritic cell by targeting c-Fos, J. Lipid Res. 53 (11) (2012) 2355–2363.

[45] J.H. Yen, V.P. Kocieda, H. Jing, D. Ganea, Prostaglandin E2 induces matrix metalloproteinase 9 expression in dendritic cells through two independent signaling pathways leading to activator protein 1 (AP-1) activation, J. Biol. Chem. 286 (45) (2011) 38913–38923.

[46] C.E. Clark, M. Hasan, P. Bousso, A role for the immediate early gene product c-fos in imprinting T cells with short-term memory for signal summation, PLoS One 6 (4) (2011) e18916.

[47] Y. Wu, M. Borde, V. Heissmeyer, M. Feuerer, A.D. Lapan, J.C. Stroud, D.L. Bates, L. Guo, A. Han, S.F. Ziegler, D. Mathis, C. Benoist, L. Chen, A. Rao, FOXP3 controls regulatory T cell function through cooperation with NFAT, Cell 126 (2) (2006) 375–387.

[48] S.C. Warth, K.P. Hoefig, A. Hiekel, S. Schallenberg, K. Jovanovic, L. Klein, K. Kretschmer, K.M. Ansel, V. Heissmeyer, Induced miR-99a expression represses Mtor cooperatively with miR-150 to promote regulatory T-cell differentiation, EMBO J. 34 (9) (2015) 1195–1213.